First publ. in: Journal of Biological Chemistry 283 (2008), 7, pp. 4124-4132

Dynamics of Trigger Factor Interaction with Translating Ribosomes*[S]

Anna Rutkowska[‡], Matthias P. Mayer[‡], Anja Hoffmann[‡], Frieder Merz[‡], Beate Zachmann-Brand[‡], Christiane Schaffitzel[§], Nenad Ban[§], Elke Deuerling[‡1], and Bernd Bukau[‡2]

From the [‡]Zentrum für Molekulare Biologie Heidelberg, University of Heidelberg, Heidelberg 69120, Germany and [§]Institut für Molekularbiologie und Biophysik, ETH Zürich, CH-8093 Zürich, Switzerland

In all organisms ribosome-associated chaperones assist early steps of protein folding. To elucidate the mechanism of their action, we determined the kinetics of individual steps of the ribosome binding/release cycle of bacterial trigger factor (TF), using fluorescently labeled chaperone and ribosome-nascent chain complexes. Both the association and dissociation rates of TF-ribosome complexes are modulated by nascent chains, whereby their length, sequence, and folding status are influencing parameters. However, the effect of the folding status is modest, indicating that TF can bind small globular domains and accommodate them within its substrate binding cavity. In general, the presence of a nascent chain causes an up to 9-fold increase in the rate of TF association, which provides a kinetic explanation for the observed ability of TF to efficiently compete with other cytosolic chaperones for binding to nascent chains. Furthermore, a subset of longer nascent polypeptides promotes the stabilization of TF-ribosome complexes, which increases the half-life of these complexes from 15 to 50 s. Nascent chains thus regulate their folding environment generated by ribosome-associated chaperones.

To promote the folding of cytosolic proteins to the native state, cells employ a large arsenal of chaperones, some of which transiently associate with ribosomes. These specialized chaperones are optimally positioned to interact co-translationally with the emerging nascent polypeptides, which allows them to assist early folding steps during ongoing synthesis thereby providing a link between translation and protein folding (1–3). In *Escherichia coli*, ribosome-associated trigger factor (TF)[3] is the first chaperone that interacts with nascent polypeptides as they emerge from the peptide exit tunnel (4–6). TF is composed of three domains, which adopt an extended shape (7, 8). The N-terminal domain provides the ribosome-binding site (9); the second domain, located at the distal end of the TF molecule opposite to the ribosome binding domain, constitutes a peptidylprolyl isomerase domain with structural homology to FK506-binding proteins (4, 10); and the C-terminal domain; builds the center of the molecule with two protruding extensions.

TF interacts with ribosomes and nascent polypeptides in a dynamic binding/release cycle (3, 11). It associates in a 1:1 stoichiometry with ribosomes via its N-terminal ribosome-binding motif, using ribosomal protein L23 as its docking site (12, 13). This initial step of the TF functional cycle is essential for its *in vivo* activity in chaperoning nascent polypeptides (13) and is accompanied by a conformational change within the chaperone (11, 13). The affinity of TF for vacant ribosomes is rather low with a dissociation constant on the order of 1 μM (14–16). However, the presence of a nascent polypeptide results in an up to 10-fold increase in affinity of TF for ribosomes (17). The half-life of TF complexes with vacant ribosomes is ~11 s and does not seem to be affected by the ongoing translation (11, 14). After dissociation from the ribosome, TF has the ability to stay associated with the growing polypeptide for a few more seconds depending on the hydrophobicity of the nascent chain. However, the detailed kinetics of TF-ribosome interactions and the parameters of the nascent chains that make the critical contributions to these interactions remain unknown.

To elucidate the mechanism of these early steps of chaperone-assisted folding of newly synthesized proteins, we investigated whether the properties of the nascent polypeptide chains, such as length, amino acid composition, and folding status affect the dynamics of TF binding to the ribosome. For this purpose, we developed a method to isolate quantitative amounts of homogeneous populations of ribosome-nascent chain (RNC) complexes, and we determined the association and dissociation rates of TF binding to these ribosomes. Our analysis revealed that the nature of nascent polypeptides significantly affects the association and dissociation rates of the TF-ribosome complex. Therefore, nascent chains control the func-

* This work was supported by Deutsche Forschungsgemeinschaft Grant SFB638 (to B. B. and E. D.), Human Frontier Science Programs (to E. D. and N. B.), a Heisenberg fellowship from the Deutsche Forschungsgemeinschaft (to E. D.), a fellowship from the Boehringer Ingelheim Fonds (to A. H.), and by a grant from the Fonds der Chemischen Industrie (to B. B.), by the Swiss National Science Fundation (SNSF), the National Center of Excellence in Research (NCER) Structured Biology program of the SNSF, and the ETH Research grant TH-3104-1 (to N. B.). The costs of publication of this article were defrayed in part by the payment of page charges. This article must therefore be hereby marked "*advertisement*" in accordance with 18 U.S.C. Section 1734 solely to indicate this fact.

[S] The on-line version of this article (available at http://www.jbc.org) contains supplemental Experimental Procedures, Figs. 1 and 2, Table 1, and additional references.

[1] To whom correspondence may be addressed. Tel.: 49-6221-546795; Fax: 49-6221-545894; E-mail: e.deuerling@zmbh.uni-heidelberg.de.

[2] To whom correspondence may be addressed. Tel.: 49-6221-546795; Fax: 49-6221-545894; E-mail: bukau@zmbh.uni-heidelberg.de.

[3] The abbreviations used are: TF, trigger factor; RNC, ribosome-nascent chain; F-TF, trigger factor-R14C mutant protein labeled with BADAN; ICDH, isocitrate dehydrogenase; RpoB, RNA polymerase subunit β; MetK, *S*-adenosylmethionine synthetase; aa, amino acid; BADAN, 6-bromoacetyl-2-dimethyl-aminonaphthalene.

tional cycle of chaperone machinery that assists the early steps of protein folding.

EXPERIMENTAL PROCEDURES

Design of Arrested Nascent Chain Constructs—See Supplemental Material for details.

Purification of Ribosomes and RNCs—Ribosomes were purified from strain MC4100 Δ*tig* as described (18). RNCs used for kinetics measurements were purified from *E. coli* strain BL21(DE3) Δ*tig*, which contained one of the arrested nascent chain plasmids (pBAT-Strep3-SecM) and the pZA4 plasmid. Strains were grown at 30 °C to an A_{600} of 0.6–0.8 in Luria-Bertani (LB) medium supplemented with 100 μg/ml ampicillin and 50 μg/ml spectinomycin. The culture was induced with 1 mM isopropyl β-D-thiogalactopyranoside and grown as before for an additional 60 min. Afterward the cells were cooled on ice, harvested by centrifugation, and frozen in liquid nitrogen. Cell pellets from 1 liter of LB medium were thawed on ice and resuspended in 10 ml of cold Buffer I (50 mM Hepes-KOH, pH 7.5, 100 mM KOAc, 12 mM $Mg(OAc)_2$, 1 mM dithiothreitol) supplemented with 1 mM phenylmethylsulfonyl fluoride. After cell lysis by French press, cell debris was removed by centrifugation (16,000 rpm, 4 °C, 2 times for 30 min). Cleared extract was adjusted to a final concentration of 1 M KOAc and 12 mM $Mg(OAc)_2$ in a final volume of 15 ml and loaded onto a 45-ml high salt sucrose cushion (25% w/v sucrose, 50 mM Hepes-KOH, pH 7.5, 1 M KOAc, 12 mM $Mg(OAc)_2$, 1 mM dithiothreitol). Bulk ribosomes were pelleted by centrifugation (44,000 rpm, 4 h, 4 °C) in a Ti45 rotor (Beckman) and resuspended overnight on ice in Buffer I supplemented with 1 mM phenylmethylsulfonyl fluoride. Resuspended ribosomes were incubated for 30 min at 4 °C with 1.5 ml of 50% *Strep*Tactin® suspension (IBA GmbH) previously equilibrated with Buffer I. Afterward, the *Strep*Tactin® resin was washed with 10 ml of Buffer I supplemented with ATP (end concentration 5 mM) and with 10 ml of Buffer I without ATP. RNCs were then eluted with Buffer I containing 2.5 mM desthiobiotin and 1 mM phenylmethylsulfonyl fluoride (6 times, 380-μl fractions), and the concentration of RNCs was determined by measuring the absorption at 260 nm. RNCs containing fractions were frozen in liquid nitrogen and stored at −80 °C. Aliquots were analyzed by SDS-PAGE and Western blotting.

For pulldown experiments, RNCs were purified from wild type BL21(DE3) strain as above omitting the ATP wash step. Elution fractions were pooled and analyzed by SDS-PAGE and Western blotting.

Purification of TF Variants—The plasmids coding for the TF-R14C and TF-FRK/AAA-R14C were constructed by site-directed mutagenesis of pDS56-TF and pDS56-TF-FRK/AAA, respectively. For site-specific labeling, 6-bromoacetyl-2-dimethyl-aminonaphthalene (BADAN, Molecular Probes) was used. See Supplemental Material for protein purification and labeling method.

Kinetic Measurements between BADAN-R14C-TF and Ribosome/RNC—All kinetic measurements were performed in Buffer F (10 mM $MgCl_2$, 6 mM β-mercaptoethanol, 20 mM Tris-HCl, pH 8.0) with all components pre-equilibrated to 20 °C by following the change in fluorescence at 507 nm with an excitation wavelength of 398 nm (7 or 7.5 nm bandwidth) in an LS55 luminescence spectrometer (PerkinElmer Life Sciences).

Association reactions were initiated by adding the ribosome or RNC-containing solution to the labeled TF variant in the fluorimeter cuvette with short manual mixing. The measurements for the TF·RNC complex formation were performed according to pseudo first-order conditions, with constant RNC concentrations (50 nM, for RNC-3-Strep also 100 nM) and titration of BADAN-R14C-TF (from 150 to 800 nM). On average for one experimental set-up, 12 association reactions were measured with eight different TF concentrations. The traces were analyzed as single exponential functions by using the program GraFit 5.0.12. The second-order association rate constant was determined by linear regression analysis of the replotted observed rates *versus* the BADAN-R14C-TF concentration. The reported values are average ± S.E. of at least four independent titrations. The measurements for the association of TF to vacant ribosomes were performed with constant ribosome concentrations (varying between experiments from around 250 to 650 nM) and titration of BADAN-R14C-TF around the given ribosome concentration (*i.e.* for 380 nM ribosomes, 300, 350, 400, and 450 nM TF). The second-order association rate constant was obtained by performing a global fit of the general solution (Equation 1) of the differential equation of the association reaction to each set of traces with constant ribosome concentration and different TF concentrations using nonlinear regression analysis and the GraphPad Prism 4.0 program (GraphPad Software, San Diego). The reported values are averages ± S.E. of at least five independent titrations weighted with their individual standard errors.

$$F = F_0 + (F_{max} - F_0) \times \frac{-2k_1[A](1 - e^{-t\sqrt{\Delta}})}{(k_1[A] + k_1[B] + k_2)(1 - e^{-t\sqrt{\Delta}}) + \sqrt{\Delta}(1 + e^{-t\sqrt{\Delta}})} \quad \text{(Eq. 1)}$$

where k_1 indicates second-order association rate constant; k_2 indicates dissociation rate constant; $[A]$ and $[B]$ indicate concentrations of BADAN-R14C-TF and vacant ribosomes, respectively, with $[A] \geq [B]$; $\Delta = (k_1[A] + k_1[B] + k_2)^2 - 4k_1^2[A][B]$.

To determine the dissociation rate constants, a 10-fold excess of unlabeled TF was added to a preformed complex of BADAN-R14C-TF and ribosomes or BADAN-R14C-TF and RNC, and the fluorescence change was recorded as described above. A single exponential function was fitted to the data using the program GraFit 5.0.12 or GraphPad Prism 4.0. For each construct the reported values are average ± S.E of at least 10 independent displacement reactions weighted with their individual standard errors. The half-life was calculated using average dissociation rate constant. The apparent dissociation equilibrium constants were calculated as the ratio between the apparent dissociation and association rate constants. In control experiments, the BADAN-R14C-TF-AAA mutant deficient in ribosome binding was used instead of BADAN-R14C-TF.

RESULTS

Design and Purification of Stalled RNC Complexes—To determine the individual parameters of nascent polypeptides

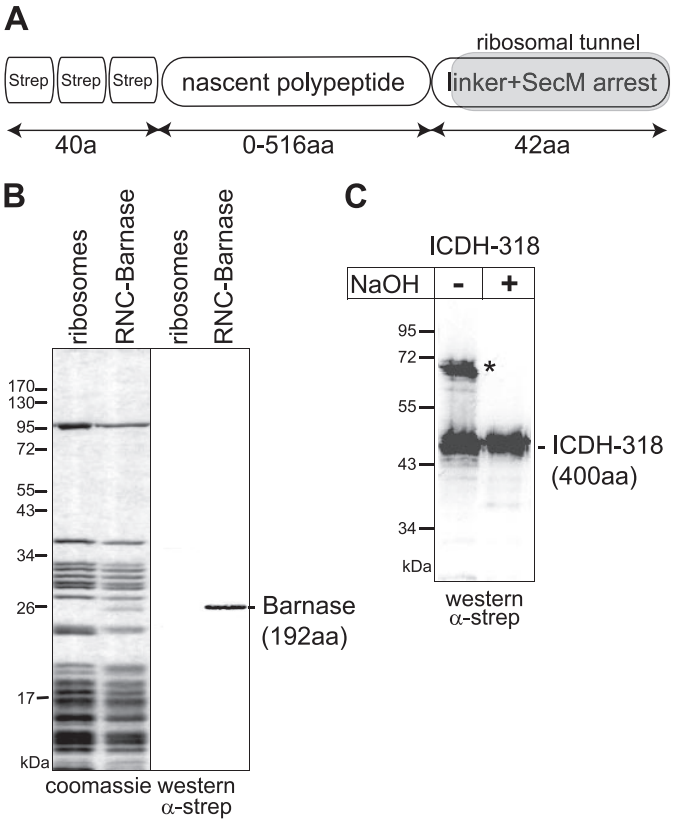

FIGURE 1. **Design and purification of RNC complexes.** *A,* schematic representation of the tested arrested nascent chains. The portion of the nascent chain buried in the ribosomal tunnel is marked in *gray*. The triple strep tag and the linker are not indicated in the name of the nascent chains, and the number of aa in the name reflects only the length of target polypeptide. *B,* SDS-PAGE of isolated vacant ribosomes and RNCs exposing Barnase detected by Coomassie staining and Western blotting using *Strep*Tactin conjugated to alkaline phosphatase; samples were treated with NaOH to release nascent chains from the peptidyl tRNA. *C,* SDS-PAGE separation of RNC-ICDH-318 detected by Western blotting as described above. The majority of purified RNCs represented monosomes because no shorter polypeptides, reflecting polysomes, were detectable. NaOH treatment, which releases the nascent chain from the peptidyl t-RNA, is indicated; the peptidyl-tRNA is marked with an *asterisk*.

that may affect the binding of TF to ribosome, it is essential to investigate RNCs harboring defined states of nascent chains, and hence to arrest the translation process at selected stages. For this purpose, we improved a method that allows the stalling of nascent chains in *E. coli* cells followed by the isolation of quantitative amounts of stalled RNCs (19, 20). To induce translational arrest, we genetically fused the 3′-end of the open reading frames of target genes to a linker encoding both the SecM peptide, which induces translational arrest (21), and additional amino acids (aa) to allow the complete exposure of the target protein at the ribosomal exit site (Fig. 1*A*) (18). In order to affinity purify the stalled RNCs, we introduced a triple strep tag sequence at the 5′-end of the gene construct (20). These fusion proteins were expressed in Δ*tig* mutant cells lacking TF resulting in the production of stalled RNCs. The isolated RNCs fractions were highly pure (Fig. 1*B* and supplemental Fig. 1), devoid of vacant ribosomes, and mainly represented monosomes that carry the nascent polypeptide of the expected size (Fig. 1*C* and supplemental Fig. 1). All purified samples were examined by immunoblotting for the presence of chaperones (GroEL, DnaK, DnaJ, and GrpE) or other ribosome-associated factors (signal recognition particle). Only in a few samples two chaperones (GroEL and DnaJ) could be detected in very small amounts (<1% compared with nascent chains) (supplemental Fig. 1*C*).

In order to investigate the kinetics of TF interaction with RNCs, we produced a set of different nascent polypeptides designed to probe both the effects of chain length and folding state. Nascent chains of various lengths were derived from two natural TF substrates, isocitrate dehydrogenase (ICDH, 416 aa) and RNA polymerase subunit β (RpoB, 1342 aa) (22). We generated RNCs exposing, in addition to the triple strep tag, either the N-terminal 27, 66, 108, 177, or 318 aa of ICDH (ICDH-27 to ICDH-318) or the N-terminal 23, 36, 100, 148, 190, 233, 325, or 516 aa of RpoB (RpoB-23 to RpoB-516). None of the ICDH derived nascent chains should be capable of adopting a compactly folded structure as judged from its atomic structure (23) and the finding that several truncated ICDH nascent chains are highly protease-sensitive (18). For RpoB, the structural features of two homologs (24, 25) suggest that RpoB-148 may fold into the first N-terminal RpoB domain and RpoB-516 encompasses the first two domains of RpoB. This conclusion is supported by proteinase K digest experiments of purified RNCs revealing an enhanced stability for RpoB-148 compared with RpoB-100 (Fig. 4*B*).

Finally, the SecM peptide used for arresting nascent chains at the ribosome is short and remains buried in the ribosomal tunnel. Therefore, the likelihood that the SecM peptide affects the folding of the exposed nascent chain is highly unlikely. Indeed, in biochemical and structural studies (see Ref.19 and data not shown), no major influence of the SecM peptide on the folding of arrested nascent chains was noticed. In addition, since all our nascent chains were constructed in the same way, potential influences of the SecM peptide and the strep tag should not interfere with the relative differences between the kinetic values.

Nascent Polypeptides Accelerate TF Association with Ribosomes—The association and dissociation kinetics of TF interactions with ribosomes and RNCs were measured using fluorescence spectroscopy. The TF variant TF-R14C was fluorescently labeled with BADAN at position Cys-14, which allowed us to monitor the ribosome binding of TF by detection of a decrease in fluorescence emission (11, 14). The addition of 0.35 μM BADAN-labeled TF (F-TF) to 0.5 μM vacant ribosomes led to a significant decrease in fluorescence emission (Fig. 2, *A* and *B*). However, no change in fluorescence was observed when the ribosome concentration was decreased to 0.05 μM. In contrast, addition of 0.05 μM RNCs carrying either ICDH-108 or RpoB-100 to 0.35 μM F-TF was sufficient to generate a strong decrease in fluorescence emission (the emission maximum remained unchanged, ~507 nm). The observed fluorescence changes specifically monitored the association of TF with vacant ribosomes and RNCs, because addition of a fluorescence-labeled TF mutant protein, F-TF-AAA, which is deficient in ribosome binding (13), to vacant ribosomes or RNCs did not result in any fluorescence change (Fig. 2*B*). Furthermore, in the absence of ribosomes, the addition of a short peptide as well as folded proteins (glyceraldehyde-3-phosphate dehydrogenase and dihydrofolate reductase) at 3 μM concen-

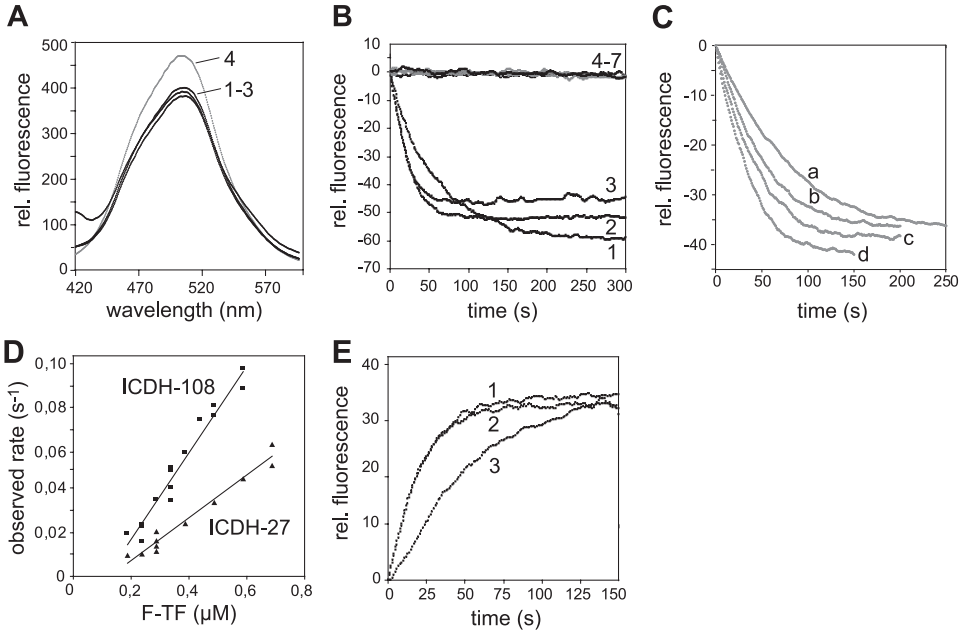

FIGURE 2. **Nascent chains modulate the association and dissociation kinetics of TF with ribosomes.** *A,* fluorescence spectra of 0.35 μM F-TF in the absence (*gray line*; *4*) and the presence of 0.5 μM vacant ribosomes (*1*) or 0.05 μM RNCs of ICDH-108 (*2*) or RpoB-100 (*3*) monitored by fluorescence emission using 398 nm excitation wavelength. *B,* kinetics of the association between 0.35 μM F-TF and 0.5 μM vacant ribosomes (*1*) or 0.05 μM RNCs of ICDH-108 (*2*) or RpoB-100 (*3*) monitored by fluorescence emission at 507 nm using 398 nm excitation wavelength. The *gray curve* represents 0.35 μM F-TF alone (*4*). In the control experiments, 0.35 μM F-TF-AAA was incubated alone or mixed with 0.5 μM ribosomes or 0.05 μM RNC of ICDH-108 (*5–7*, respectively). *C,* representative association curves for TF·RNC complex formation. Time course of the association of 0.05 μM RNCs exposing ICDH-66 with 0.2, 0.25, 0.3, and 0.35 μM F-TF (*a–d,* respectively). *D,* dependence of the observed association rates for RNCs of ICDH-108 and ICDH-27 on F-TF concentration. *E,* kinetics of dissociation monitored by displacement experiment: 0.35 μM F-TF was competed from its complex with 0.5 μM vacant ribosomes (*1*) or 0.05 μM RNCs exposing ICDH-108 (*2*) or RpoB-100 (*3*) by adding 3.5 μM unlabeled TF. For the simplicity, first 150 s of dissociation reaction are shown, which was on average monitored for 200 s. A single exponential equation was fitted to the association and dissociation data as detailed in supplemental Fig. 2.

trations had no effect on the F-TF fluorescence (data not shown). All labeled TF proteins used in our experiments were functionally similar to unlabeled wt-TF as judged from chaperone assays with denatured glyceraldehyde-3-phosphate dehydrogenase (data not shown), which is in agreement with earlier characterizations of F-TF (11, 14).

In order to determine the rates of TF association with vacant ribosomes and RNCs, we varied F-TF concentrations from 150 to 700 nM, while keeping the concentrations of ribosomes (0.5 μM) or RNCs (0.05 μM) constant. The observed association rates, obtained from such a F-TF titration experiment, increases as a function of increasing concentrations of F-TF, and all kinetics are best described by mono-exponential functions (Fig. 2*C*). The determined second-order association rate constants are highly reliable as demonstrated by linear regression analysis of the replotted observed rates *versus* the F-TF concentration, resulting in an excellent fit of the data points to a linear correlation (examples given in Fig. 2*D*). The association rate (k_{on}) of TF interaction with vacant ribosomes was 21×10^3 M^{-1} s^{-1}. However, the presence of a nascent chain increased this association rate of F-TF in case of all tested polypeptides (supplemental Table 1). To test for any contribution of the N-terminal strep tag, we determined the association rate of F-TF to RNCs exposing only the tag sequence (RNC-3-Strep). This tag increased the association rate of the chaperone by 2.4-fold compared with vacant ribosomes (Fig. 3).

The Length of Nascent Polypeptides Affects TF Association with Ribosomes—We next examined the influence of nascent chain length on the association rates of F-TF to ribosomes. For RNCs exposing ICDH chains, the rates gradually increased with increasing chain length up to 8.6-fold above vacant ribosomes for the ICDH-108 construct. For RNCs exposing even longer chains of ICDH (ICDH-177 and ICDH-318), the association rates decreased again to 5.2- and 4-fold above empty ribosomes, respectively (Fig. 3 and supplemental Table 1). In the case of RNCs exposing RpoB chains, the association rate increased more than 7-fold upon exposure of only 36 N-terminal aa of RpoB (RpoB-36) and gradually decreased for RpoB-190 to RpoB-516 down to 2.5-fold in comparison to vacant ribosomes (Fig. 3 and supplemental Table 1). Notably, the association rate of F-TF with the RpoB-148 nascent chain, which may be capable of folding into a stable subdomain, was lower than the next shorter and longer polypeptides, RpoB-100 and RpoB-190, respectively. Nascent chains of two other model TF substrates, *S*-adenosylmethionine synthetase (MetK) and firefly luciferase, caused comparably strong effects on the association rate of TF with ribosomes (Fig. 3 and supplemental Table 1).

In summary, the interaction of F-TF with the tested sets of RNCs showed the same tendency as follows: a chain length-dependent increase in the association rate, up to almost 9-fold, followed by a decrease for RNCs exposing very long chains (approximately >200 exposed aa). An increase in chain length generally goes along with an increase in the number of hydrophobic patches that define TF-binding sites as determined by peptide array analysis of several protein sequences, including ICDH (22, 26). The occurrence and composition of such hydrophobic stretches are likely to be the major determinants for stimulating TF binding to RNCs (Fig. 3*B*). This is evident for RpoB-36, harboring an extended contiguous hydrophobic stretch of 13 aa, in comparison with a slightly short nascent chains of RpoB (RpoB-23, Fig. 3) in which this stretch is absent. These chains differ only by a few amino acids in length, but they display different k_{on} of approximately 163,000 and 95,000 $M^{-1}s^{-1}$, respectively. The subsequent decrease of the association rates for the RNCs exposing long ICDH and RpoB nascent chains (Fig. 3) most likely reflects the increased capacity of the nascent chains to attain

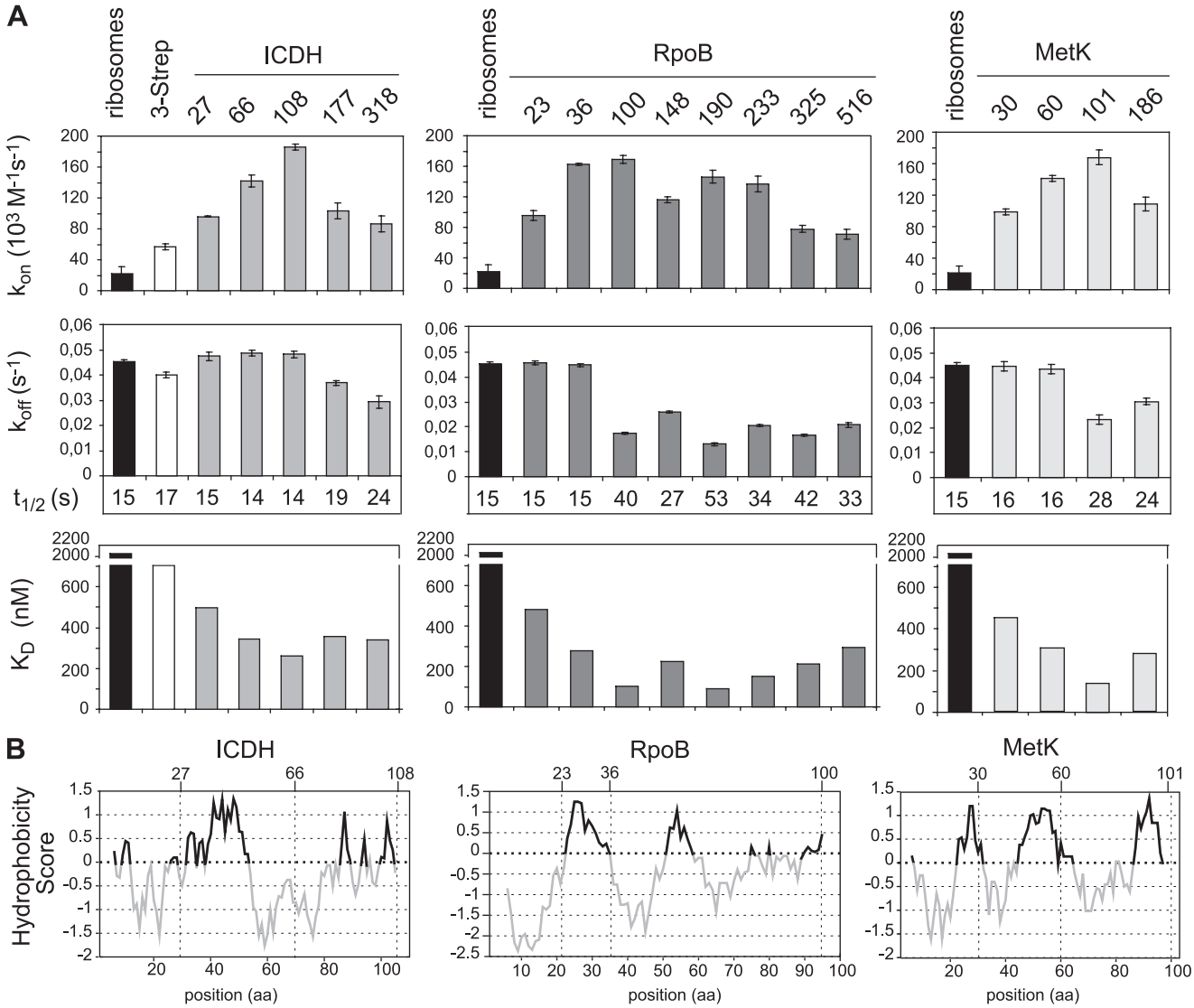

FIGURE 3. **Length of the nascent chain affects TF binding to ribosomes.** *A,* kinetics of TF interactions with RNCs exposing nascent chains of different length (ICDH, *gray*; RpoB, *dark gray*; MetK, *light gray*). Controls: vacant ribosomes (*black*), RNC-3-Strep (*white*). The reported values for the association rate constants (k_{on}) are the average of at least three independent titration experiments; for the dissociation rate constants (k_{off}), the reported values are the average of at least eight displacement reactions; the half-life ($t_{1/2}$) was calculated from the average k_{off} value; the apparent dissociation equilibrium constants (K_D) were calculated as the ratio between the apparent dissociation and association rate constants. Errors are given as the means ± S.D. See supplemental Table 1for more details. *B,* regions of high hydrophobicity (*black line*) along the sequence of short nascent chains derives from ICDH, RpoB, and MetK. The hydrophobicity plots were made with ProtScale program (ExPASy) using the hydropathy scale by Kyte-Doolittle and averaging over a window of 11 residues.

some secondary and tertiary structure, resulting in the burying of TF-binding sites.

Folding States of Nascent Polypeptides Influence TF Association with Ribosomes—The observed decrease in the association rates for longer chains or partially folded domains (RpoB-148) suggested that the folding state of a nascent polypeptide may influence TF binding to ribosomes. To test this directly, we investigated two additional pairs of RNCs, each of which contains nascent chains of similar length and sequence but different folding state. The first set consisted of folded α-spectrin SH3-wt domain (62 aa) and a mutant derivative, SH3-m10, that can only adopt a random coil structure due to two point mutations (27). SH3-m10 remains protease-sensitive when exposed as arrested polypeptide on the surface of ribosomes (18). The second set consists of a full-length Barnase mutant (110 aa), which is deficient in RNase activity but can properly fold (28), and a truncated Barnase variant (Barnase-95, 95 aa), which lacks its C-terminal 15 aa. We found that while ribosome-tethered Barnase can adopt a fold that confers protease resistance, Barnase-95 remains protease-sensitive suggesting that it is incapable of adopting any significant native-like structure (Fig. 4*A*), which is consistent with earlier results of *in vitro* folding studies (29). Although the two SH3-wt and SH3-m10 nascent chains are identical in length and differ by only two amino acids, they exhibited differences in the TF association rates. The k_{on} for TF binding to RNCs carrying unfolded SH3-m10 was 1.6-fold higher than RNCs carrying folded SH3-wt (Fig. 5 and supplemental Table 1). We observed very similar results for Barnase and Barnase-95 RNCs. These data support the hypothesis that folding of the nascent chain retards TF binding to ribosomes. Nevertheless, folded Barnase and SH3-wt nascent chains showed enhanced TF association rates compared with

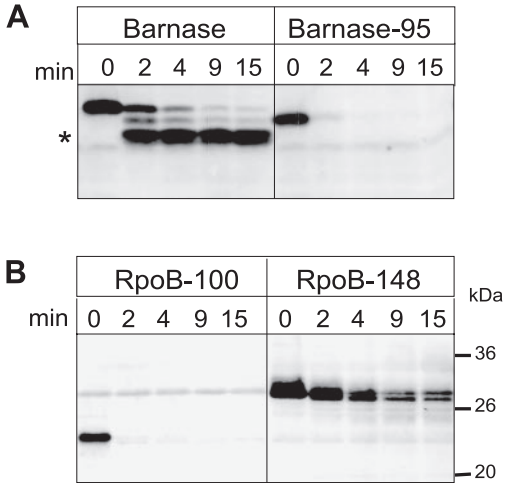

FIGURE 4. **Purified RNCs exposed nascent chains of different folding status.** In order to investigate folding state of nascent polypeptide, proteinase K was added to *ex vivo* purified RNCs: *A,* Barnase and Barnase-95; *B,* RpoB-100 and RpoB-148, and at indicated time points of the digest (0, 2, 4, 9, and 15 min) degradation was stopped. Polypeptides were separated by SDS-PAGE and visualized by Western blotting using monoclonal antibody against the SecM arrested sequence. The degradation product marked with an *asterisk* in *A* represents Barnase without the triple strep tag, which was confirmed using *Strep*Tactin® conjugated to alkaline phosphatase (data not shown).

vacant ribosomes, suggesting that TF can accommodate and has significant affinity for globular domains of small size. The stimulation of TF binding to these substrates may result from the presence of hydrophobic patches that are exposed on the surface of the native folds (30, 31).

Nascent Polypeptides Delay TF Dissociation from Ribosomes—We next determined the dissociation rates (k_{off}) of TF from vacant ribosomes and RNCs by monitoring the loss of quenching of the fluorescence signal when a 10-fold molar excess of unlabeled TF was added to preformed F-TF·RNC complexes. Fig. 2*E* depicts representative results for RNCs harboring ICDH-108 or RpoB-100 and vacant ribosomes. For RNCs exposing various lengths of ICDH, SH3-m10, and the folded SH3-wt and Barnase, the TF dissociation rates were affected to only a minor extent compared with vacant ribosomes. In contrast, nascent chains of RpoB and Barnase-95 significantly decreased the TF dissociation rate compared with vacant ribosomes (Figs. 3 and 5). Importantly, this effect was observed exclusively for longer nascent chains: whereas the dissociation rates for TF from RNC carrying RpoB-23 and RpoB-35 and from vacant ribosomes were similar, RpoB-100 up to RpoB-516 decreased the k_{off} by up to 3.5-fold. Comparable results were obtained for two other nascent polypeptides, MetK and firefly luciferase (Fig. 3 and supplemental Table 1). As soon as the nascent chain can adopt a compactly folded structure, the k_{off} increased as shown for Barnase and its unfolded mutant version Barnase-95. These results indicate that nascent chains, dependent on their length, sequence, and folding status, can stabilize the TF·RNC complexes by increasing the half-life ($t_{½}$) of the complex from 15 to 53 s.

Nascent Polypeptides Increase the Affinity of TF for Ribosomes—The determination of the ribosome association and dissociation rates of F-TF allowed us to calculate the apparent dissociation equilibrium constants (K_D) for these interactions. The K_D

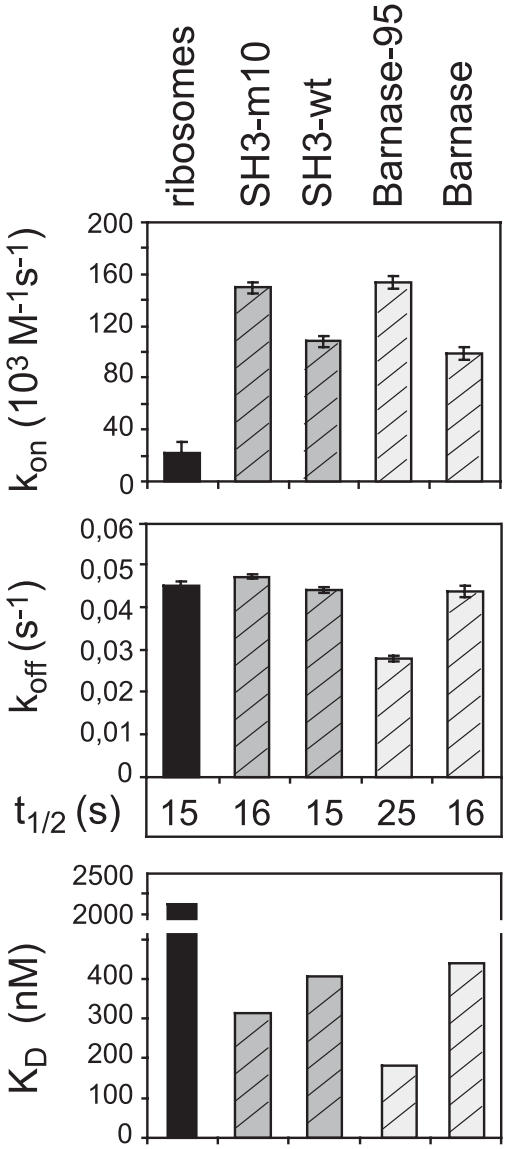

FIGURE 5. **Folding state of the nascent chain affects TF binding to ribosomes.** Kinetics of TF interactions with RNCs exposing nascent chains of different folding status (SH3-m10 and SH3-wt, *dark gray hatched*; Barnase-95 and Barnase, *light gray hatched*). Control, vacant ribosomes (*black*). Data were collected and analyzed as described in Fig. 3.

of F-TF to vacant ribosomes is 2.1 μM, which is in agreement with earlier reports (11, 14–17). All tested RNCs exhibited a substantial decrease in the K_D, ranging from 4.3-fold for the short ICDH-27 nascent chain to ~26-fold for the long RpoB-190 nascent chain (Fig. 3). In case of ICDH, the increase in affinity was caused solely by an increased association rate. In contrast, the increased association rates as well as the decreased dissociation rates for RpoB contributed to the increase in affinity of TF for ribosomes. For all tested sets of RNCs, TF affinity to ribosomes eventually decreased for long nascent polypeptides due to a decrease in the association rates. As expected, also the folding status of the nascent chain affected the interaction of TF with RNCs. The affinity of TF for ribosomes exposing a small folded domain (SH3-wt or Barnase) at the ribosomal exit site was lower compared with ribosomes carrying unfolded polypeptide chains of similar length (Fig. 5).

Additionally, we analyzed the co-purification of TF with RNCs exposing different lengths of SecM-arrested nascent chains isolated from wild type *E. coli* cells. For most of the RNCs used in this study, we could observed the correlation between the efficiency of TF co-purification and the determined K_D (data not shown). Finally, the obtained very high affinities for RNCs carrying short RpoB nascent chains are in agreement with previous results (17).

DISCUSSION

The folding environment for nascent polypeptide chains that is generated by ribosome-associated chaperones is of decisive importance for protein biogenesis. This is evident by the severe protein aggregation and lethality phenotype of *E. coli* mutants lacking both TF as well as DnaK system, which presumably backs up TF to rescue misfolded proteins (32, 33). To understand the mechanism of the early stages of protein folding, we dissected the kinetic rates of the various steps in the functional cycle of TF. Our strategy was to arrest translation at defined steps and determine the dependence of the individual kinetic parameters of the TF-ribosome interaction cycle on the status of the nascent chains.

Here we show that the nascent chains, dependent on their length, sequence, and folding status, significantly accelerate TF association with ribosomes and can delay its dissociation. In this way the nascent chains themselves control the interaction of TF with the ribosome, the critical step that is essential for TF activity in chaperoning the folding of newly synthesized proteins (13, 34). Nascent polypeptide chains thus serve as timer for the interaction of TF with ribosomes (Fig. 6).

The presence of nascent polypeptide chains increased the association rates of TF with its ribosomal binding site by 3- to 9-fold (Fig. 6). Our results, obtained from several sets of nascent chains derived from different proteins (ICDH, RpoB, firefly luciferase, and MetK), show that the increase in association rates correlates with increased length of nascent chains, which in turn correlates with the number of hydrophobic stretches. The individual contributions of these parameters are difficult to dissect.

We note that the association rates eventually decrease for RNCs exposing either very long chains (approximately ≥200 exposed aa) or folded domains (SH3, Barnase, RpoB-148). It is likely that folding of the nascent chains reduces the rate at which TF binds the ribosome, presumably by burying hydrophobic residues serving as TF-binding sites. In addition, the increasing size of the nascent chains may sterically hinder TF from binding to L23 (Fig. 6*D*). However, the observed differences in the association rates of TF to RNCs carrying folded and unfolded nascent chains (SH3, Barnase) are surprisingly modest (approximately by 33%). This finding indicates that TF can associate with significant affinity even with folded globular domains.

How can nascent polypeptides accelerate the association of TF with its ribosomal binding site? How can TF be faithfully targeted to RNCs rather than to unfolded proteins in the cytosol for which it also has affinity? The affinity of TF for both vacant ribosomes and unfolded proteins is similarly low (1 μM) (14, 15, 35). The kinetics of these interactions are, however,

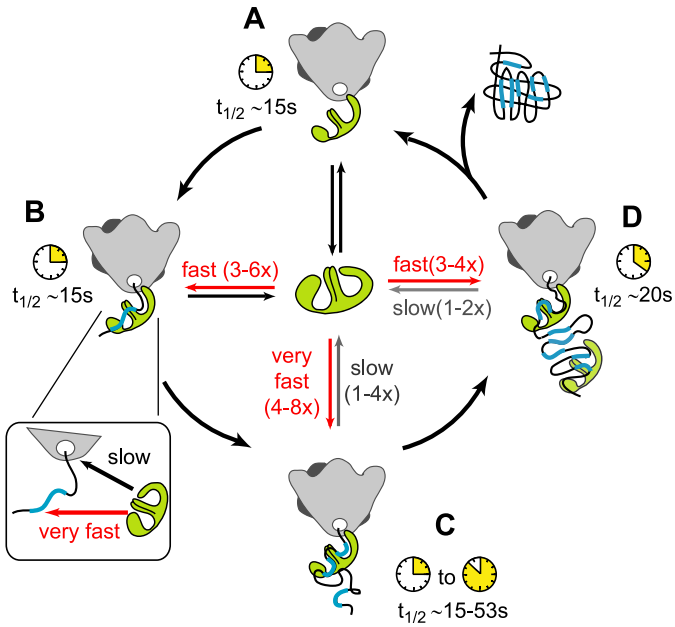

FIGURE 6. **Model of the dynamic cycle of TF interaction with ribosomes.** *A* and *B*, TF (*green*) association with ribosomes is accelerated when a peptide chain emerges from the ribosomal exit tunnel. *C*, some longer nascent chains can additionally stabilize the TF·ribosome complex up to a half-life ($t_{1/2}$) of 53 s. *D*, association rate of TF for ribosomes eventually decreases when a large nascent polypeptide is exposed on the ribosomal surface. TF may remain associated with some nascent chains even after dissociation of TF from its ribosomal binding site (11). Hydrophobic stretches serving as possible TF-binding sites are marked in *blue*. See text for further details.

completely different. TF has rather low association and dissociation rates for ribosomes but very high association and dissociation rates for unfolded proteins (14, 35). This ability to rapidly bind and release unfolded polypeptides may allow TF to sample for binding sites on the growing nascent chain (Fig. 6*B*). We propose that the presence of TF-binding sites on nascent chains in proximity of the ribosomal exit tunnel increases the local concentration of TF, thereby targeting TF to its ribosomal binding site. Kinetically speaking, the nascent chains increase the association rate, and thereby the affinity of TF to ribosomes. By such a mechanism, TF can discriminate between vacant ribosomes, translating ribosomes and unfolded polypeptides. Moreover, the initiation of the chaperone cycle of TF is accelerated immediately when a new peptide chain emerges from the ribosomal exit tunnel. Furthermore, it allows, in principle, the rapid reloading of TF to RNCs after dissociation of the initially bound TF during ongoing protein synthesis. Such cycling may be in particular relevant for the assisted folding of large-sized multidomain proteins, which are the preferred clients for TF *in vivo* (22, 32). Finally, these properties provide a kinetic explanation for the observed ability of TF to efficiently compete with other cytosolic chaperones for binding to nascent chains. Nascent polypeptides stimulate binding of TF to ribosomes by up to a $k_{on} = 200 \times 10^3\ M^{-1}\ s^{-1}$. This rate is comparable to the association rates of the downstream acting chaperone DnaK (in its ATP-bound form) and its co-chaperone DnaJ (that targets DnaK to its substrates) to unfolded proteins (36, 37). Taking into account that the cellular concentration of TF (~50 μM) is 2- and 60-fold higher than those of DnaK and DnaJ, respectively, these association rates would ensure that TF is the first

chaperone to interact with nascent polypeptides (12, 33, 38, 39). Thus, the nascent chain may also play a crucial role in establishing the sequential order in the mode of action of the cytosolic chaperones. The prior binding of TF to translating ribosomes does not exclude, however, that the DnaK and GroEL chaperones may associate with some of the longer nascent chains simultaneously to TF.

In addition our analysis indicates that a subset of nascent polypeptide chains modulates the dissociation of TF from translating ribosomes by decreasing the k_{off} up to 3-fold as compared with vacant ribosomes (Fig. 6*C*). The dissociation rates are decreased only for non-native nascent chains exposing $\geq$100 residues, a trend observed for almost all tested proteins, the most prominent of which were RpoB and Barnase-95. This stabilization of the TF·RNC complexes is likely to result from the increase in number of hydrophobic binding sites that are accessible for TF interactions. Our observation that nascent polypeptide chains can stabilize the TF·ribosome complex ($t_{1/2}$ increases from 15 to ~53 s) suggests that there is no intrinsic, invariant timer that dictates the half-life of the TF·ribosome complex.

What might be the consequences of an increased half-life of TF·RNC complexes? The prolonged ribosome binding of TF may allow the accumulation of longer nascent chain segments in association with this chaperone. This may be a prerequisite for influencing their folding states and assisting the formation of long distant interactions within domains.

With respect to the obtained association and dissociation rates, it should be considered that in the cell during ongoing translation the dynamics of TF interaction with ribosomes (i) will be continuously changing through the whole range of measured values because the nascent protein will increase in length and change its propensity for folding during the chaperoning cycle, and (ii) it can be additionally modified by molecular crowding. Nevertheless, the obtained data show the following trend: upon the start of translation, TF immediately binds to ribosomes, and the formed TF·ribosome complex can be stabilized by the nascent chain, which may play a crucial role for synthesis of multidomain proteins or when the translation process slows down.

In summary, our kinetic analysis complements the recent study from Hartl and co-workers (11) describing the steady-state kinetics of TF interactions during translation. The novel aspects added by our study are as follows: (i) to show that nascent chains increase the rate of TF association with ribosome, thereby providing a kinetic explanation for the ability of TF to select translating ribosomes and to efficiently compete with other cytosolic chaperones for binding to nascent chains; (ii) to describe the kinetic range by which different types of nascent chains influence TF association with ribosomes, which is a critical step for the chaperone activity of TF; (iii) to demonstrate that nascent chains are capable of controlling the dissociation kinetics of TF·RNC complexes, thus allow the fine-tuning of the chaperone cycle for the particular needs of individual chains. In contrast to the results presented here, the half-life of TF·ribosome complexes under steady-state conditions ($t_{1/2}$ ~ 11 s) was determined to be unaffected during ongoing translation (11). This apparent discrepancy could be the result of the different experimental set-ups. The steady-state measurements during ongoing translation investigate the effects of heterogeneous ensemble of nascent chains, comprising all stages from short to long length. Therefore, this method does not detect the individual contributions of nascent chains of different lengths on the half-life of the TF·ribosome complex. On the other hand, our results do not exclude that TF may remain associated with growing polypeptides even after it has dissociated from the ribosome (Fig. 6*D*), as proposed by Kaiser *et al.* (11). Our experimental set-up does not allow detection of such interactions. Both mechanisms, prolonged association of TF with translating ribosome and prolonged association of TF with nascent chains, may be important for TF to prevent misfolding and assist early folding steps during translation. Together, both studies provide a more comprehensive framework for understanding the mechanism of TF chaperone action at the ribosome.

Acknowledgments—We thank members of the Bukau and Deuerling laboratories, in particular D. Huber and G. Kramer, for comments on the manuscript. We also thank L. Serrano and A. Matouschek for their generous gifts of plasmids.

REFERENCES

1. Young, J. C., Agashe, V. R., Siegers, K., and Hartl, F. U. (2004) *Nat. Rev. Mol. Cell Biol.* **5,** 781–791
2. Frydman, J. (2001) *Annu. Rev. Biochem.* **70,** 603–647
3. Bukau, B., Deuerling, E., Pfund, C., and Craig, E. A. (2000) *Cell* **101,** 119–122
4. Stoller, G., Ruecknagel, K. P., Nierhaus, K. H., Schmid, F. X., Fischer, G., and Rahfeld, J.-U. (1995) *EMBO J.* **14,** 4939–4948
5. Valent, Q. A., Kendall, D. A., High, S., Kusters, R., Oudega, B., and Luirink, J. (1995) *EMBO J.* **14,** 5494–5505
6. Hesterkamp, T., Hauser, S., Lutcke, H., and Bukau, B. (1996) *Proc. Natl. Acad. Sci. U. S. A.* **93,** 4437–4441
7. Ludlam, A. V., Moore, B. A., and Xu, Z. (2004) *Proc. Natl. Acad. Sci. U. S. A.* **101,** 13436–13441
8. Ferbitz, L., Maier, T., Patzelt, H., Bukau, B., Deuerling, E., and Ban, N. (2004) *Nature* **431,** 590–596
9. Hesterkamp, T., Deuerling, E., and Bukau, B. (1997) *J. Biol. Chem.* **272,** 21865–21871
10. Hesterkamp, T., and Bukau, B. (1996) *FEBS Lett.* **385,** 67–71
11. Kaiser, C. M., Chang, H. C., Agashe, V. R., Lakshmipathy, S. K., Etchells, S. A., Hayer-Hartl, M., Hartl, F. U., and Barral, J. M. (2006) *Nature* **444,** 455–460
12. Lill, R., Crooke, E., Guthrie, B., and Wickner, W. (1988) *Cell* **54,** 1013–1018
13. Kramer, G., Rauch, T., Rist, W., Vorderwülbecke, S., Patzelt, H., Schulze-Specking, A., Ban, N., Deuerling, E., and Bukau, B. (2002) *Nature* **419,** 171–174
14. Maier, R., Eckert, B., Scholz, C., Lilie, H., and Schmid, F. X. (2003) *J. Mol. Biol.* **326,** 585–592
15. Patzelt, H., Kramer, G., Rauch, T., Schönfeld, H. J., Bukau, B., and Deuerling, E. (2002) *Biol. Chem.* **383,** 1611–1619
16. Raine, A., Ivanova, N., Wikberg, J. E., and Ehrenberg, M. (2004) *Biochimie* (*Paris*) **86,** 495–500
17. Raine, A., Lovmar, M., Wikberg, J., and Ehrenberg, M. (2006) *J. Biol. Chem.* **281,** 28033–28038
18. Hoffmann, A., Merz, F., Rutkowska, A., Zachmann-Brand, B., Deuerling, E., and Bukau, B. (2006) *J. Biol. Chem.* **281,** 6539–6545
19. Evans, M. S., Ugrinov, K. G., Frese, M. A., and Clark, P. L. (2005) *Nat. Meth.* **2,** 757–762
20. Schaffitzel, C., and Ban, N. (2007) *J. Struct. Biol.* **158,** 463–471
21. Nakatogawa, H., and Ito, K. (2002) *Cell* **108,** 629–636

22. Deuerling, E., Patzelt, H., Vorderwülbecke, S., Rauch, T., Kramer, G., Schaffitzel, E., Mogk, A., Schulze-Specking, A., Langen, H., and Bukau, B. (2003) *Mol. Microbiol.* **47,** 1317–1328
23. Hurley, J. H., Thorsness, P. E., Ramalingam, V., Helmers, N. H., Koshland, D. E., Jr., and Stroud, R. M. (1989) *Proc. Natl. Acad. Sci. U. S. A.* **86,** 8635–8639
24. Campbell, E. A., Pavlova, O., Zenkin, N., Leon, F., Irschik, H., Jansen, R., Severinov, K., and Darst, S. A. (2005) *EMBO J.* **24,** 674–682
25. Cramer, P., Bushnell, D. A., and Kornberg, R. D. (2001) *Science* **292,** 1863–1876
26. Patzelt, H., Rudiger, S., Brehmer, D., Kramer, G., Vorderwulbecke, S., Schaffitzel, E., Waitz, A., Hesterkamp, T., Dong, L., Schneider-Mergener, J., Bukau, B., and Deuerling, E. (2001) *Proc. Natl. Acad. Sci. U. S. A.* **98,** 14244–14249
27. Blanco, F. J., Angrand, I., and Serrano, L. (1999) *J. Mol. Biol.* **285,** 741–753
28. Mossakowska, D. E., Nyberg, K., and Fersht, A. R. (1989) *Biochemistry* **28,** 3843–3850
29. Neira, J. L., and Fersht, A. R. (1999) *J. Mol. Biol.* **285,** 1309–1333
30. Musacchio, A., Noble, M., Pauptit, R., Wierenga, R., and Saraste, M. (1992) *Nature* **359,** 851–855
31. Mauguen, Y., Hartley, R. W., Dodson, E. J., Dodson, G. G., Bricogne, G., Chothia, C., and Jack, A. (1982) *Nature* **297,** 162–164
32. Deuerling, E., Schulze-Specking, A., Tomoyasu, T., Mogk, A., and Bukau, B. (1999) *Nature* **400,** 693–696
33. Teter, S. A., Houry, W. A., Ang, D., Tradler, T., Rockabrand, D., Fischer, G., Blum, P., Georgopoulos, C., and Hartl, F. U. (1999) *Cell* **97,** 755–765
34. Agashe, V. R., Guha, S., Chang, H. C., Genevaux, P., Hayer-Hartl, M., Stemp, M., Georgopoulos, C., Hartl, F. U., and Barral, J. M. (2004) *Cell* **117,** 199–209
35. Maier, R., Scholz, C., and Schmid, F. X. (2001) *J. Mol. Biol.* **314,** 1181–1190
36. Gamer, J., Multhaup, G., Tomoyasu, T., McCarty, J. S., Rüdiger, S., Schönfeld, H.-J., Schirra, C., Bujard, H., and Bukau, B. (1996) *EMBO J.* **15,** 607–617
37. Siegenthaler, R. K., and Christen, P. (2006) *J. Biol. Chem.* **281,** 34448–34456
38. Tomoyasu, T., Ogura, T., Tatsuta, T., and Bukau, B. (1998) *Mol. Microbiol.* **30,** 567–581
39. Mogk, A., Tomoyasu, T., Goloubinoff, P., Rüdiger, S., Röder, D., Langen, H., and Bukau, B. (1999) *EMBO J.* **18,** 6934–6949